



POLİTEKNİK DERGİSİ

JOURNAL of POLYTECHNIC

ISSN: 1302-0900 (PRINT), ISSN: 2147-9429 (ONLINE)

URL: <http://dergipark.gov.tr/politeknik>



Experimental verification of cell shape-collapse relationships in metallic foams by photoelasticity method

Metalik köpüklerin hücre biçimi-çökme ilişkisinin fotoelastisite metodu ile deneysel olarak doğrulanması

Yazar(lar) (Author(s)): Ersin BAHCECI¹, Yusuf OZCATALBAS²

ORCID¹: 0000-0002-7719-6051

ORCID²: 0000-0002-4256-8492

Bu makaleye şu şekilde atıfta bulunabilirsiniz (To cite to this article): Bahceci E. and Ozcatalbas Y., "Experimental verification of cell shape-collapse relationships in metallic foams by photoelasticity method", *Politeknik Dergisi*, 22(4): 1101-1110, (2019).

Erişim linki (To link to this article): <http://dergipark.gov.tr/politeknik/archive>

DOI: 10.2339/politeknik.490993

Experimental Verification of Cell Shape-Collapse Relationships in Metallic Foams by Photoelasticity Method

Araştırma Makalesi / Research Article

Ersin BAHCECI^{1*}, Yusuf OZCATALBAS²

¹İskenderun Technical University, Faculty of Engineering and Natural Science, Department of Metallurgical and Materials Engineering 31200-İskenderun/Hatay, Turkey

²University of Gazi, Faculty of Technology, Department of Metallurgical and Materials Engineering 06500-Besevler/Ankara, Turkey

(Geliş/Received : 30.11.2018 ; Kabul/Accepted : 11.02.2019)

ABSTRACT

In the present study, the effect of cell morphology on mechanical properties in metallic foams with Al based closed cells was examined. AlSi8Mg0.8 alloyed metallic foam materials were produced by the Powder Metallurgy (PM) method. The elastic stresses and their distributions which were created by the compression load in the metallic foams, producing in similar density and different cell sizes were investigated by the photoelasticity method. The fracture and collapse mechanisms of the foaming materials, having the same density but different cell size and shape factor, exhibited discrepancy as well. The elastic stress concentrations and their distributions that were created by compression at the cell walls could be determined by the photoelasticity method. It was detected that the fringe orders in the photoelasticity images provided important and accurate information about the stress concentration areas at the foam walls. It was specified that the collapse at the end of the compression tests started mostly at these areas.

Keywords: Metallic foam, cell morphology, photoelasticity, stress distribution, collapse.

Metalik Köpüklerin Hücre Biçimi-Çökme İlişkisinin Fotoelastisite Metodu ile Deneysel Olarak Doğrulanması

ÖZ

Bu çalışmada, Al esaslı kapalı hücreli metalik köpüklerdeki hücre morfolojisinin mekanik özellikler üzerindeki etkisi incelenmiştir. AlSi8Mg0.8 alaşımlı metalik köpük malzemeler Toz Metalurjisi (PM) yöntemiyle üretilmiştir. Benzer yoğunlukta ve farklı hücre boyutlarındaki metalik köpüklerde basma yükü ile oluşturulan elastik gerilmeler ve bunların dağılımları fotoelastisite yöntemi ile incelenmiştir. Aynı yoğunlukta fakat farklı hücre boyutu ve şekil faktörüne sahip köpük malzemelerin kırılma ve çökme mekanizmaları da farklılık göstermiştir. Hücre duvarlarında basma ile oluşturulan elastik gerilme konsantrasyonları ve dağılımları fotoelastisite yöntemiyle belirlenebilmiştir. Fotoelastisite görüntülerdeki renk saçaklarının (fringe orders) köpük duvarlarındaki gerilme yığılma bölgeleri hakkında önemli ve doğruluğu yüksek bilgi verdiği tespit edilmiştir. Basma deneyleri sonunda çökmenin çoğunlukla bu bölgelerde başladığı belirlenmiştir.

Anahtar Kelimeler: Metalik köpük, hücre morfolojisi, fotoelastisite, gerilim dağılımı, çökme.

1. INTRODUCTION

Foam materials have attracted attention in recent years as materials used in various engineering practices. They have the ability to be considerably deformed by constant stress [1, 2]. Although intensive researches continue on the metallic foams, the effect of cell structure on the foam characteristics could not be explained clearly. The most important reason is the cell structure which cannot be controlled entirely during the production of foam

materials. Therefore, the cell structure shows a difference in the foam materials having the same chemical composition and same mechanical properties. It is known that the relative density of the cell wall directly affect the mechanical properties of the foams when compared to their thickness [3]. Elasticity modules, densities and cell morphology of the foams should be defined to find usability of lots of industrial application.

There are publications in the related literature about cell fractures of metallic foams and calculations of their strength [4, 5]. With mechanical tests, performing tensile-compression operation strength can be determined [4, 6, 7]. It is used in micromechanical models in predicting cell breakage [8]. In addition, non-

*Sorumlu yazar (Corresponding Author)
e-posta : ersin.bahceci@iste.edu.tr

destructive, mathematical modeling has been developed in computational and principal component analysis techniques using cell shapes [8-10]. Also, work has already been done to give an idea about where to collapse and how breaks will start [11].

In this study, analyzability of effect of cell morphology of metallic foam with closed cell, which is produced by powder metallurgy method, on the stresses occurring on cell walls and mechanical properties of the foam was investigated using photoelasticity method. This method was used at the first time for Aluminum foams in the present study. Photoelasticity is the non-destructive stress measuring technique commonly used for measuring stresses through unit deformations on the surface during static or dynamic tests conducted on a piece or a structure. In this method, firstly the test piece is coated with a special resin susceptible to unit deformation. Afterwards, test or service loads are applied on the piece. Coating is illuminated through the polarized light coming from the polariscope. Colors shown on the coating with the help of the polariscope demonstrate the distribution of stresses and high stress areas. Color

changes are recorded through continuous recording [12, 13]. The greatest advantage of this method is the capability to measure the elastic stresses on industrial parts under service conditions without the need for creating a model. Elastic deformations and their corresponding stresses can be calculated according to various colors shown on the surface examined by optical devices [13, 14].

2. EXPERIMENTAL STUDIES

2.1. Material and Method

%8Si+%0.8Mg+%1.2 TiH₂ (by weight) and the remaining Al powder % were mixed in Turbula and pressed in room temperature under 300 MPa pressure and this way the block samples were obtained (Figure 1). The properties of the powder used in the sample production rates are given in Table 1. After sintering block samples at 500 °C (15 minutes) they were extruded at 400 °C. Extruded sample was rolled gradually at 400 °C and plate shaped preform materials (that can be foamed) were produced.

Table 1. Production and properties of the powder used in the sample rates.

Material	Al	Si	Mg	TiH ₂	Alloy
Chemical composition (% by weight)	Remainder	8	0,8	1,2	-
Purity (%)	99,9	99,9	99,95	-	-
Grain size (µm)	<160	<20	<150	<45	-
Dissociation temperature (°C)	-	-	-	480-570	-
Melting point (°C)	660	1414	650	-	632

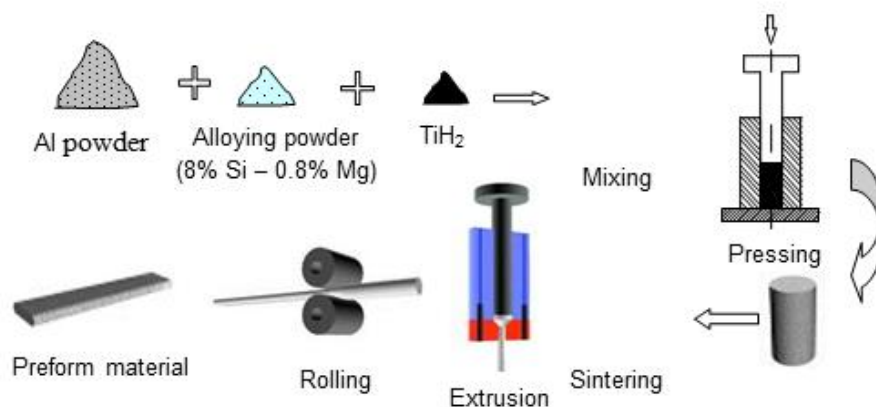


Figure 1. Preform foam material processing steps.

Theoretical density of the block samples produced was calculated as 2.68 g/cm³. The density increased up to 2.65 g/cm³ after the deformation caused by the hot extrusion applied to the sintered material and the density reaching up to 99% was achieved. The maximum density achieved with the rolling process after the extrusion was 99.3%.

Figure 2 illustrates SEM image of the extruded sample. It was seen that light grey particles in EDS analysis were TiH₂; and black particles were Si. Certain circled zones were rich in Mg. It is thought that black particles in these zones shown in Al matrix involved the Mg particles decomposed and Mg₂S precipitates during the extrusion process. It was observed that the deformation processes did not have any significant effect on homogeneous dispersion of TiH₂ and Si particles but the deformation texture became more explicit with especially the rolling process (Figure 3) [15].

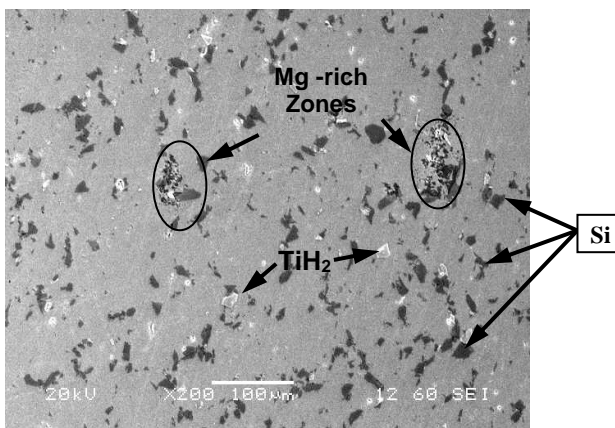


Figure 2. Microstructure of the extruded sample

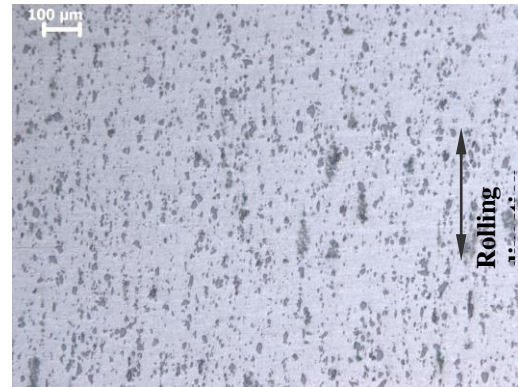


Figure 3. Microstructure of rolled sample.

After being kept at the foaming temperature of 720 °C for about 15 minutes, the metallic foam which filled the mould cavity was taken with the mould out of the furnace and left for cooling in the circulating air. At the end of the process, block foam samples and photoelasticity test samples (Figure 4) were prepared. In the present study, the foaming mould that has high heat transfer coefficient was used in order to provide a heat transfer between the Al foam and the mould surface [16].

Figure 4 illustrates block foam samples produced with the size of 30X25X150 mm and samples prepared for photoelasticity experiment. Block foam samples were cut into sizes of 30x25x25 mm, their open surfaces were coated with resin coating material and their photo-stress images were taken by using polariscope (Figure 4.b). Reflective adhesive materials were coated the surface as thin as possible.

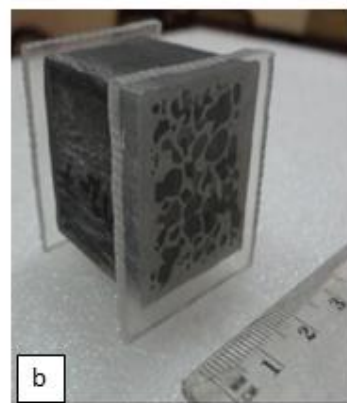
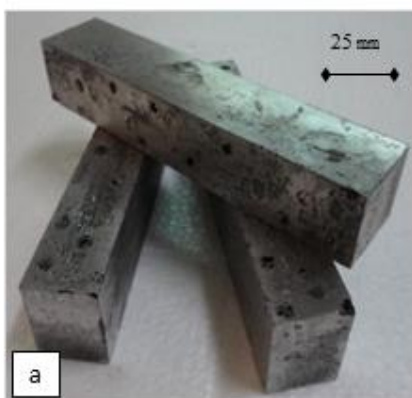


Figure 4. a) Foam blocks and b) photoelasticity sample.

Photoelasticity test apparatus is shown in Figure 5.a-b. For this purpose a compression press of 10 kN capacity was used. The applied loads were measured with a load cell connected to data logger.

In the determination of cell shape factor and size, image analysis was made from the scanning pictures of foam samples. Cell size was determined by the two dimensional cell diameter calculation method.

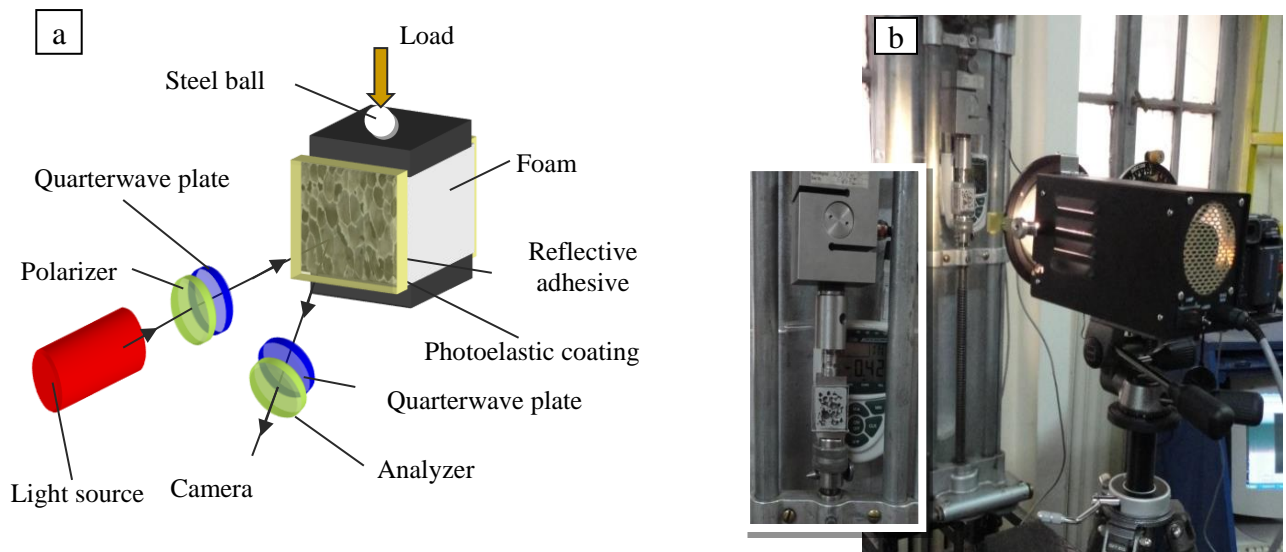


Figure 5. a) Schematic illustration of the experimental setup and b) Photoelasticity experimental setup.

2.2. Calculations of Elasticity Modulus, Density and Cell morphology

The elasticity modulus and densities with respect to the regular hexagon (Honey comb) closed cell model approach were determined using Gibson and Ashby (1997)' method. The equation is given in Eq. 1 [17, 18].

$$\frac{E^*}{E_s} = \phi^2 \left(\frac{\rho^*}{\rho_s}\right)^2 + (1-\phi) \left(\frac{\rho^*}{\rho_s}\right) \quad 1$$

Where E_s and ρ_s are the elastic modulus and mass density of solid cell wall of the foam material, ϕ is the volume fraction of solid contained in the cell edges while E^* and ρ^* are the elastic modulus, plateau stress and mass density of foam. The mechanical properties of aluminium foam of closed cell depend mainly on the uniformity, greatness, distribution and relative density of cell structures [19]. Raj and Daniel (2008), stated that there was a deficiency in the model of regular hexagon closed cell foam elasticity module given by Gibson & Ashby (1997) and made Regression analysis. Gibson and Ashby model have two parts. $(\rho^* / \rho_s)^2$ and (ρ^* / ρ_s) represent the cell wall and cell side effects respectively (Eq 1).

$$\text{Shape factor}(F) = \frac{4\pi}{n} \sum_i^n \frac{a_i}{l_i^2} \quad 2$$

Where, n = total number of cells, i = cell number, a_i = cell area and l_i = cell-boundary length. The shape factor described the deviation of the cell geometry foam a circle with $F= 1$. It is found that F decreases much more with decreasing foam density than expected from the transition of spherical to polygonal cells. Ideally the foam structure to the shape factor is regarded to be approximately 0.9 [20].

3. RESULTS AND DISCUSSION

3.1. Foam material

Microstructure pictures of the cell walls of the material after the foaming are given in Figure 6. Co-axial α -Al dendrites phase, Al-Si eutectic phase and primary Si phase were observed on the figures. It was seen that the primary Si was still in the structure. It meant that Si could not change the structure as eutectic because it did not find enough time and the solidification process was too fast depending on the faster heat loss. The Si phase was generally solidified in plate-like cell walls [21]. The structure showed great similarity with the literature finding [22-24].

It was shown that the strain localization in the latter stages of deformation was present in both foam types: Broad deformation bands caused a collective collapse of cell walls were observed in pure Al foam. Whereas characteristic brittle fracture of the AlSi12 foam matrix resulted in distinctive, highly localized bands [25].

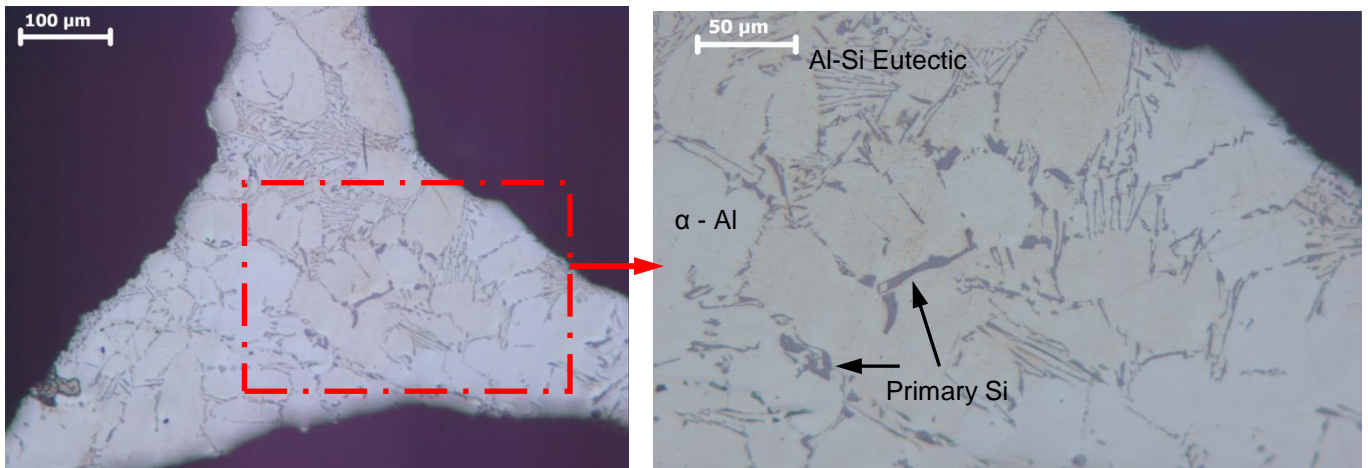


Figure 6. Foam plateau and cell wall microstructure (5% etching).

The general characteristics of foam materials that were produced in three different density group and different average cell sizes are shown in Table 2. In general, nearly spheroidal and uniform cell distribution was observed. The highest 0.78 shape factor value was reached. Cell

wall breakups and cell extinctions were seen in the areas in contact with the mould surface. Metallic foams with uniform cell size and distribution were produced having narrowing standard deviation interval with the decreasing average cell dimension.

Table 2. General physical and geometrical characteristics of foam materials.

Average Density (g/cm ³)	Foam material	Density - ρ (g/cm ³)	Average cell size -d (mm)	Cell standard deviation (δ)	Shape factor (F)
MFI- 0.62	MF1	0.62	2.9	0.84	0.71
	MF2	0.60	3.3	0.92	0.72
	MF3	0.65	3.6	1.34	0.74
MFII -0.70	MF4	0.70	3.1	0.71	0.78

The metallic foam sample produced an average cell size, standard deviation intervals and distributions is shown to Figure 7. They were produced standard deviation range

narrowed uniform cell size and distribution, increased number of cells and decreasing average cell size.

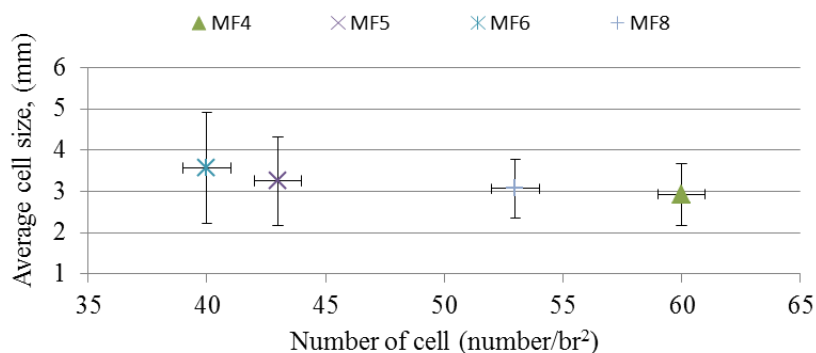


Figure 7. Foam cell sizes and their distribution.

3.2. Photoelasticity test results

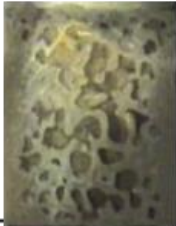
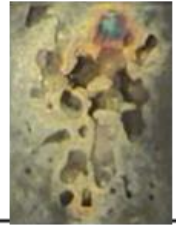

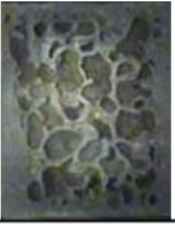



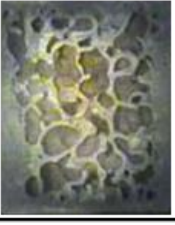



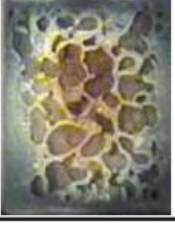



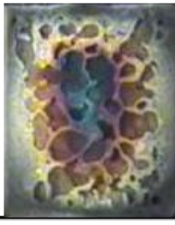








Significant data, on images taken using Vishay PALC 3 Photostress program, with high accuracy rates were

determined on the elastic stress accumulation areas and degrees of foam materials [21]. On photoelastic images, the color fringe orders creating color transitions were obtained with the increase of load (and therefore stress).

It was observed that different tones of the same colors (color degree) increased in direct proportion to the increasing stress.

In the photoelastic images, fringe orders that create colour passages with the increase of load were obtained. It was specified that the fringe orders increased directly with the increasing of load (Table 3).

Table 3. Load-Photoelasticity changes with respect to foam type.

	Elastic module (GPa)			
Gibson & Ashby	6.7	6.5	7.1	11.8
Load (kN)	MF1	MF2	MF3	MF4
0.25				
0.50				
0.75				
1.00				
1.25				
1.50				

10 mm



During the compression tests, created elastic stress on cell walls was measured within elastic limits by photoelasticity method. Up to the yield stress, there was no significant effect on the mechanical failure of the adhesive material holding the photoelastic coatings (lids) on both sides. The function of the adhesive material is to transfer the elastic strain in the cell walls to the lids. However, it was observed that the strength of the cell walls was affected by the photoelastic coatings after the yield strength. For this reason, the lids were removed by means of a non-destructive technique and also the compression process was continued.

During 0.25 kN loading no colour change was observed in MF4 material whereas in the MF2 material formation

of fringe orders was seen (stress concentration area) (Table 3). In the MF4 material with the increasing load the fringe orders were at the first degree at 1 kN whereas the equivalent image to this image on the MF2 material was observed at 0.25 kN load and on a narrower area. Similar relation was also seen in the MF3 and MF1 materials. The elastic loadings which were applied to metallic foams caused stress concentrations according to the cell shapes in the structure. Depending on the increase of the force lines, the stress also increased proportionally. Regular colour outlook meant regularly distributed stress areas [26]. In the foam materials, the significant photoelastic images were obtained according to the classification of the elastic module values of Gibson model.

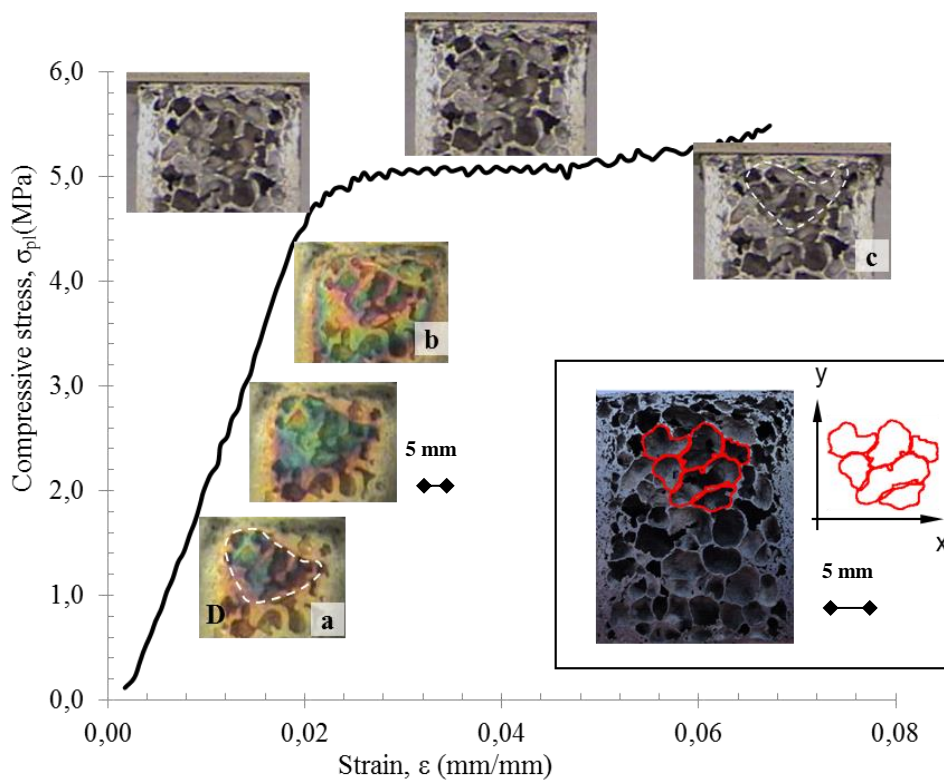


Figure 8. The stress-strain curve of MF1 foam a-b)Photoelastic image, c) Collapsing deformation in compression test.

Figure 8.a shows that the stress concentration was more intensive (at the area D of the photoelastic image of MF1). In Figure 8.c, it was observed that firstly the plateau and walls were collapsed as expected [27]. It was

specified that as the stress concentration image was being observed on the top areas of foam, the fringe orders proceeded towards the bottom areas of foam with the increase of the load (Figure 8.b).

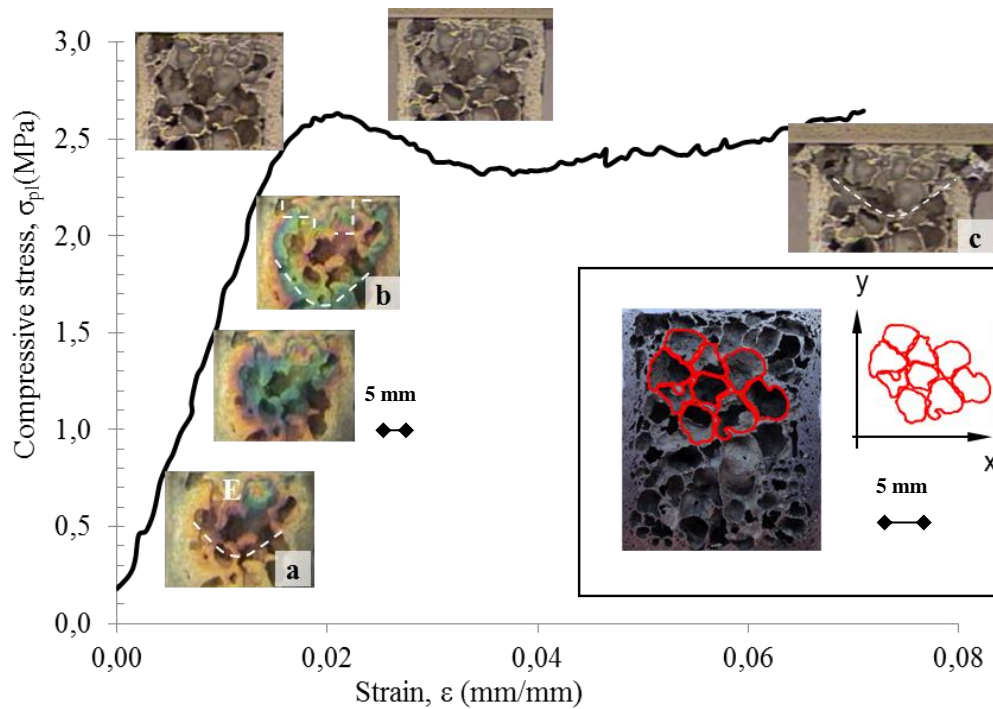


Figure 9. The stress-strain curve of MF2 foam a-b) Photoelastic image, c) Collapsing deformation in compression test.

A more intense stress accumulation was observed on the area marked with E on the photoelastic image on MF2 foam sample (Figure 9.a). The collapse was anticipated to occur on this area because of the small area and also close to foam piece's upper part. The stress accumulation occurring on the plateau area on the upper part of the big cell in the E area seen on Figure 9.c (with the decrease of

the area affected by the load) caused wedge-shaped collapses on both sides with an approximate angle of 45o in the direction that the load was applied. It was determined that the beginning areas of the collapse were the same with stress areas obtained on the photoelastic image within elastic limits.

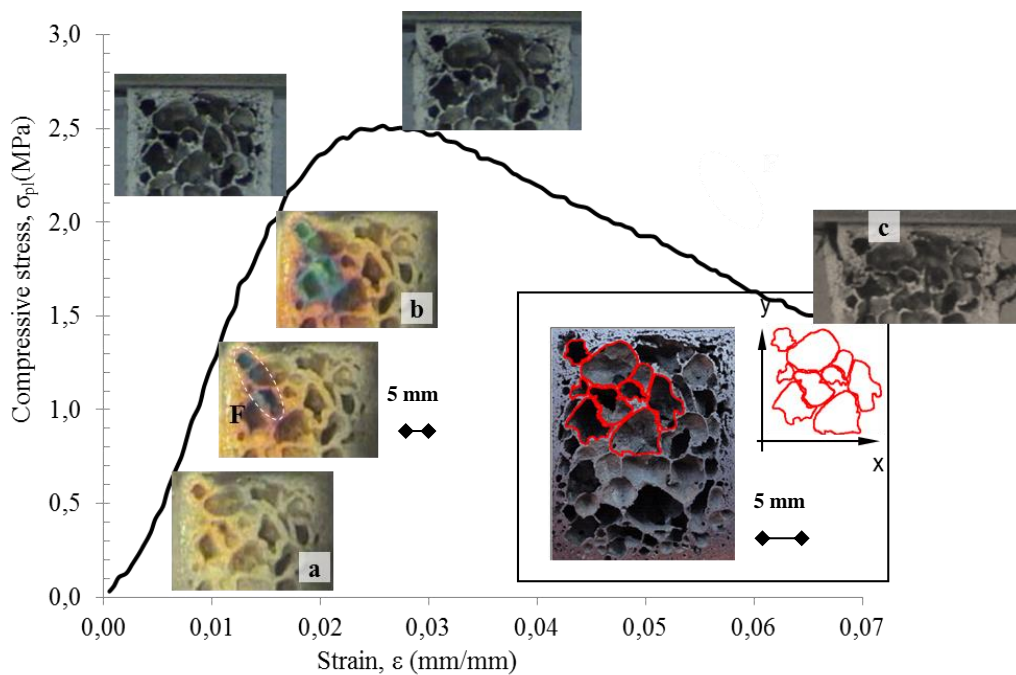


Figure 10. The stress-strain curve of MF3 foam a-b) Photoelastic image, c) Collapsing deformation in compression test.

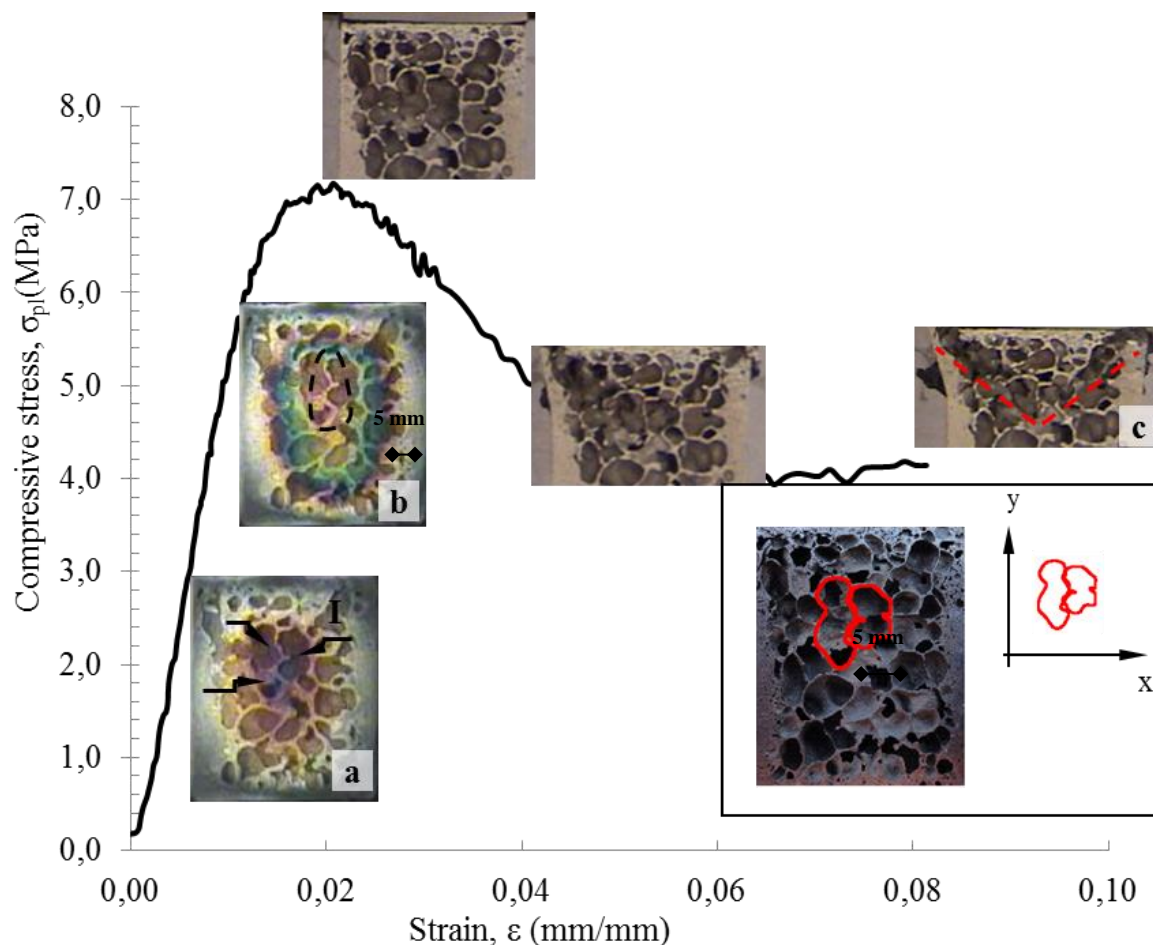


Figure 11. The stress-strain curve of MF4 foam a-b) Photoelastic image, c) Collapsing deformation in compression test.

The photoelastic image created on the MF3 foam material is given in Figure 10.a. It was seen that the stress was concentrated on the area shown as F. During the compression test it was observed that this stress area joined the first fracturing process and was realized with the deformation of cells shown in F (Figure 10.b).

It was observed on photoelastic images of MF4 foam material that stress was intense on the plateau area marked with I arrows (Figure 11). Elasticity module (E^*) and yield stress (σ_{pl}) of the foam material vary depending on the density of the foam material, cell size and distribution [17, 20]. It was observed on MF4 foam material that since thickness of cell walls and the intensity in that area were limited, elastic stress areas become centered on these areas. It was also determined on compression test process images that collapses generally started and fracture process continued on these areas. (Figure 11.c).

6. CONCLUSION

- Metallic foam production of AlSi8Mg0.8 alloy was carried out in density of $0.62 - 0.70 \text{ g/cm}^3$ and different cell sizes by powder metallurgy route.

- Alpha Al, Al-Si-eutectic and primary Si phases were seen on the microstructure of the produced metallic foam cell walls.
- Satisfactory evidences about relationship between stress concentration regions and cell shapes of metallic foams under compression loads were obtained by means of photoelasticity method.
- Formation of cell plateau collapse and cell wall fractures were observed at the intensive stresses regions determined by this method with the compression effect. Therefore, the photoelasticity method could be used to have preliminary information on the mechanical behaviour of metallic foam materials under loads.
- In the metallic foam materials, significant photoelastic image is obtained as the elastic module values increased (with respect to the Gibson model) with the change of fringe orders.
- The overall results were shown that the behaviour (collapse, breakage, etc.) of porous structures under stress in the cell walls can be predicted by using the photoelastic method.

ACKNOWLEDGEMENT

Authors thank to Gazi University providing support as BAP project.

REFERENCES

- [1] Hanssen, A.G., Langseth, M. and Hopperstad, O. S., “Static and Dynamic Crushing of Circular Aluminium Extrusions with Aluminium Foam Filler”, *Int. J. of Impact Eng.* 24(5):475-507, (2000).
- [2] Ruan, D., Lu, G., Chen, F.L., Siores, E. “Compressive Behaviour Of Aluminium Foams at Low And Medium Strain Rates”, *Composite Structures*, 57, 331–336, (2002).
- [3] Yi Y., Zheng X., Fu Z., Wang C., Xu X., and Tan X., “Multi-Scale Modeling for Predicting the Stiffness and Strength of Hollow-Structured Metal Foams with Structural Hierarchy”, *MDPI Materials*, 11(380): 1-12, (2018).
- [4] Jeon I., Asahina T., “The effect of structural defects on the compressive behavior of closed-cell Al foam”, *Acta Materialia*. 53(12): 3415-3423, (2005).
- [5] Jeon I., Katou K., Sonoda T., Asahina T., Kanga Ki-Ju., “Cell wall mechanical properties of closed-cell Al foam”, *Mechanics of Materials*. 41(1): 60-73, (2009).
- [6] Zhihua W., Hongwei M., Longmao Z., Guitong Y., “Studies on the dynamic compressive properties of open-cell aluminum alloy foams”, *Scripta Materialia*. 54(1): 83-87, (2006).
- [7] Tan P. J., Harrigan J. J., Reid S. R., “Inertia effects in uniaxial dynamic compression of a closed cell aluminium alloy foam”, *Materials Science and Technology*, 18(5): 480-488, (2013).
- [8] Marsavina L., Kováčik J., Linul E., “Experimental validation of micromechanical models for brittle aluminium alloy foam”, *Theoretical and Applied Fracture Mechanics*, 83: 11-18, (2016).
- [9] Sevostianov I., Kováčik J., Šimančík F., “Elastic and electric properties of closed-cell aluminum foams: Cross-property connection”, *Materials Science and Engineering: A*, 420(1–2): 87-99, (2006).
- [10] Mines R. A. W., “On the Characterisation of Foam and Micro-lattice Materials used in Sandwich Construction”, *Strain An International Journal For Experimental Mechanics*. 44(1): 1-83, (2008).
- [11] Singh R., Lee P. D., Lindley T. C., Kohlhauser C., Hellmich C., Bram M., Imwinkelried T., Dashwood R. J., “Characterization of the deformation behavior of intermediate porosity interconnected Ti foams using micro-computed tomography and direct finite element modeling”, *Acta Biomaterialia*, 6(6): 2342-2351, (2010).
- [12] Vishay Tech Note TN-702-2, “Introduction to Stress Analysis the PhotoStress Method”, 1–13, (2011).
- [13] Ozer, A., Ozcatalbas, Y., “Measuring the residual/permanent stresses by using hole-drilling method and calibration of rosette strain-gauges”, *J. Fac. Eng. Arch. Gazi Univ.* 26(3): 657-666, (2011).
- [14] Cevik, B., Ozer, A. ve Ozcatalbas, Y., “Analysis of Stress Generated in Fillet Welds by Using Photoelasticity Method”, *6th International Advanced Technologies Symposium (IATS'11)*, 409-414, (2011).
- [15] Bahceci, E. and Ozcatalbas, Y., “Microstructural Characterisation Of The AlSiMg Alloy Metallic Foams Produced With P/M Method”, *IN-TECH*, 459-463 (2013).
- [16] Guarino S., Di Ilio G., and Venettacci S., “Influence of Thermal Contact Resistance of Aluminum Foams in Forced Convection: Experimental Analysis”, *MDPI Materials*, 10: 1-14, (2017).
- [17] Gibson, L. J. and Ashby, M. F., “Cellular Solids: Structure and Properties-Second edition”, *Cambridge University Press*, 175-308, (1997).
- [18] Kim, A., Hasan, M.A., Nahm, S.H. and Jun, Y.D., “Compressive Mechanical Properties of Closed Cell Al-Si-Cu-Mg Alloy Foams”, *Int. conference on mechanical engineering*, 1-6, (2003).
- [19] Raj, R.E. and Daniel, B.S.S., “Structural and Compressive Property Correlation of Closed-Cell Aluminium Foam”, *Journal of Alloys And Compounds*. 467: 550-556, (2008).
- [20] Degischer, H.P. and Kriszt, B., “Handbook of Cellular Metals: Production, Processing and Applications”, *Wiley-VCH. Weinheim*, 1-363, (2002).
- [21] Bahceci, E., “Effect of cell morphology on mechanical properties of closed cell metal foams and usability of photoelasticity method”, *University of Gazi Science Enstitute*, 106-117, (2012).
- [22] Kaufman, J. Gilbert and Rooy Elwin L., “Aluminum Alloy Castings: Properties, Processes, and Applications”, *ASM International*, 120, (2004).
- [23] Nafisi S., Ghomashchi R., “Effect of modification during conventional and semi- solid metal processing of A356 Al-Si Alloy”, *Science and Engineering, A* 415: 273–285, (2006).
- [24] Apelian, D., “Aluminum Cast Alloys: Enabling Tools for Improved Performance”, *North American Die Casting Association*, 6-17, (2009).
- [25] Kádár C., Máthi K., Knapék M., and Chmelík F., “The Effect of Matrix Composition on the Deformation and Failure Mechanisms in Metal Matrix Syntactic Foams during Compression”, *MDPI Materials*, 10(196): 1-10, (2017).
- [26] Ozkir, S.E., “Photoelastic Stress Analysis of Fixed Restorations over Straight and Inclined Implants with Different Macro-Designs”, *Ankara University Graduate School Of Health Sciences*, 40-47, (2007).
- [27] Aly M. S., “Behavior of closed cell aluminium foams upon compressive testing at elevated temperatures: Experimental results”, *Materials Letters*, 61(14–15): 3138-3141, (2007).